

NEW DEVELOPMENTS IN MICROPLANE AND MULTICRACK MODELS FOR CONCRETE

I. Carol
ETSECCPB-UPC, Barcelona, Spain.

Z. P. Bažant
Dept. of Civil Engineering, Northwestern University, Evanston, IL, USA.

Abstract

Extensive studies have been devoted in recent years to the microplane and multicrack models for nonlinear behavior and cracking of concrete. A new theoretical framework that links the traditional damage and plasticity concepts with the microplane theory is presented. The multicrack model is described in terms of multisurface elastoplasticity, with emphasis on the corner problem.

1 Introduction

The idea of developing material laws for the 2-D or 3-D continuum starting from the behavior of a plane of generic orientation is old and has proven very powerful. The classical elastoplastic failure envelopes such as Tresca and Mohr-Coulomb can be derived from the idea of a limit σ - ϵ condition for a generic plane (Mohr, 1900). The slip theory of plasticity (Taylor, 1938; Batdorf and Budiansky, 1949) and the viscoplastic-type multilaminate model for fractured rocks and soils (Zienkiewicz and Pande, 1977; Pande and Sharma, 1983) were also based on similar ideas.

The application of this general idea to concrete was proposed by Bažant and Oh (1983), in the form of the microplane model. After successive

modifications (Bažant and Gambarova, 1984; Bažant and Oh, 1985) the model reached its classical formulation in Bažant and Prat (1988a,b) where it was verified successfully by comparison with most of the experimental data available for concrete specimens. Later, the model was improved to an explicit form (Carol et al., 1992b) which offered much better numerical efficiency with similar data fitting capabilities, and revised by introduction of the so-called stress-strain boundaries as well as generalization to finite strain (Bažant et al., 1995).

All these developments were based on the assumption of certain stress-strain laws for the microplanes and a micro-macro constraint of the kinematic type, which leads to the expression of the macroscopic stresses tensor as an integral over the hemisphere of the normal and shear stresses on each microplane. Damage concepts with the hypothesis of strain equivalence were introduced in Carol et al. (1991), with the result of a fourth-order damage tensor expressed as the integral of some microplane damage variables. This tensor, purely geometric in nature (i.e. totally independent from material rheology) made it possible to combine damage with linear aging viscoelasticity, and reproduce long-term failure under sustained loads as given by the Rüşh curves (Carol and Bažant, 1991; Carol et al., 1992a).

With the kinematic constraint, the strains in all microplanes must be the projections of the same macroscopic strain tensor. This means that at the constitutive level no localized deformations are allowed to exist in a single plane as it would correspond intuitively to a developing (macro)crack. This does not preclude the representation of cracking in a smooth continuous fashion, as for instance in the non-local implementation (Bažant and Ožbolt, 1990) where, using fine meshes, cracks can be obtained as the result of continuum strain accumulation across two or three (or more) finite elements. Cracking, however, cannot be easily represented in the sense of classical smeared crack band models (fixed or rotating crack), where the information about the direction and opening or sliding of the crack is available at each Gauss point. Also, the simplest regularization procedure of adjusting softening diagrams with element size, as done in the crack band model requires some model parameters to be related to the fracture energy, which cannot be done easily with the kinematically constrained formulation.

With those considerations in mind, the multicrack model was proposed (Carol and Prat, 1990), with a static constraint along the line of the original formulation of Batdorf and Budiansky (in which the stresses on each plane are projections of the macroscopic stress tensor) and accumulation of inelastic strains from each cracked plane, as proposed in previous formulations for cracking (de Borst and Nauta, 1985; Willam et al., 1987). Same as in those formulations, individual cracks start and develop with precise orientations, and their strains have a discrete character, i.e. a single crack produces measurable deformations at the macroscopic level (this is in contrast to the slip theory of plasticity or statically constrained microplane models, in which the microplane strains need to be integrated over a certain finite range of

orientations to obtain some measurable macroscopic strain). In the practical implementation, the possibility of cracking is restricted to a number of fixed predefined orientations (12 planes, every 15°, in 2D). The model conforms to multisurface plasticity, and exhibits two fracture energy parameters for mode I (tension) and mode IIa (shear and high compression). The results obtained during the first stage of development (Carol and Prat, 1991; Carol et al., 1993) included constitutive calculations under pure tension and confined compression, as well as a finite element results of a three-point bend test, all of them examples where principal directions remained fixed.

A comprehensive summary of the state-of-the-art in microplane and multicrack models at the time of FraMCoS-1 was presented in Carol et al. (1992a). Since that time, significant advances have taken place, and some of them are summarized in the following. For microplane model, a theoretical framework is presented which incorporates traditional damage and plasticity concepts into the formulation in a simple and natural fashion, encompassing at the same time the previous formulations. For the multicrack model, the formulation is described in terms of multisurface elastoplasticity. The corner problem with two or more surfaces potentially active is discussed and the algorithm used is described and demonstrated with an example of application in which principal directions rotate significantly and non-trivial patterns of crack activation and deactivation are obtained.

2 Microplane model *

2.1 Standard formulation for concrete with kinematic constraint

A microplane is any plane cutting the material, defined by its unit normal vector of components n_i . Normal and shear stresses σ_N , σ_T , and strains ϵ_N , ϵ_T , are considered on each microplane. Strains on the microplane ϵ_N , ϵ_T , are assumed equal to the projections of the macroscopic strain tensor ϵ_{ij} (kinematic constraint). Application of the principle of virtual work leads to the expression of the macroscopic stress tensor as an integral of the stress over all possible microplane orientations:

$$\sigma_{ij} = \frac{3}{2\pi} \int_{\Omega} \sigma_N n_i n_j d\Omega + \frac{3}{2\pi} \int_{\Omega} \frac{\sigma_T}{2} (n_i \delta_{rj} + n_j \delta_{ri}) d\Omega \quad (1)$$

Without the shear contribution on the right-hand side, and a stress-strain law of the type $\sigma_N = \mathcal{F}_N(\epsilon_N)$, Eq. (1) represents the first formulation considered for the microplane model, which yielded satisfactory data fits for tensile cracking and shear data (Bažant and Oh, 1985; Bažant and Gambarova, 1984). With it, however, it was not possible to obtain the type of volumetric-deviatoric interaction observed in experiments in compression. Then, the split of the normal microplane stresses and strains into volumetric

* This section is authored jointly by I. Carol and Z.P. Bažant.

and deviatoric parts ($\sigma_N = \sigma_V + \sigma_D$, $\epsilon_N = \epsilon_V + \epsilon_D$) was introduced, which lead to the alternative expression:

$$\sigma_{ij} = \sigma_V \delta_{ij} + \frac{3}{2\pi} \int_{\Omega} \sigma_D n_i n_j d\Omega + \frac{3}{2\pi} \int_{\Omega} \frac{\sigma_{T_r}}{2} (n_i \delta_{rj} + n_j \delta_{ri}) d\Omega \quad (2)$$

In the formulation with volumetric-deviatoric split, the stress-strain laws are assumed

$$\sigma_V = \mathcal{F}_V(\epsilon_V) \quad ; \quad \sigma_D = \mathcal{F}_D(\epsilon_D) \quad ; \quad \sigma_{T_r} = \mathcal{F}_{T_r}(\epsilon_{T_r}, \epsilon_V) \quad (3a, b, c)$$

In practice, for a given strain history at the macroscopic level (input), the strains in the microplanes are immediate; from these, the stresses can be obtained with the material laws, and finally macroscopic stresses are obtained with (2). Integrals over the hemisphere are performed numerically. A fixed number of “sample” directions (normally 21, 25 or 28 in 3D) are considered. They serve as integration points at which history variables for the microplane laws are stored and updated. The details of the stress-strain laws, integration rules and results obtained for a variety of concrete tests can be found in Bažant and Prat (1988b) and Carol et al. (1992b).

Although in all the references mentioned it was shown that in most loading situations the formulation with normal-deviatoric split performs satisfactorily, it has been pointed out recently that under uniaxial loading with significant tensile strains (i.e. representing tensile cracking) the intrinsic normal-deviatoric coupling causes undesirable volumetric expansion that cannot be eliminated (Bažant et al., 1994; Bažant et al., 1995). In these studies, the authors propose a model with boundary stress-strain curves that switches automatically from the formulation with split to that without split, depending on the loading situation. An alternative to this problem may be to decompose the strain into a continuous part and a cracking part, and relate to the classical microplane model only the continuous part, while the cracking part is handled directly by a cracking model along the line of the multicrack model described in Sec. 3.

2.2 Elastic behavior and double constraint

In the elastic regime, the microplane laws can be simply written as

$$\sigma_V = E_V^0 \epsilon_V \quad ; \quad \sigma_D = E_D^0 \epsilon_D \quad ; \quad \sigma_{T_r} = E_{T_r}^0 \epsilon_{T_r} \quad (4a, b, c)$$

By substituting these and the kinematic constraint into (2), and comparing (2) to the standard isotropic linear elastic stiffness tensor, one can obtain the equivalence conditions (Bažant and Prat, 1988a):

$$E_V^0 = \frac{E}{1-2\nu} \quad ; \quad E_D^0 = \eta_0 E_V^0 \quad ; \quad E_{T_r}^0 = \frac{1}{3} \left[\frac{5(1-2\nu)}{1+\nu} - 2\eta_0 \right] E_V^0 \quad (5a, b, c)$$

where E^0 and ν are the standard elastic constants, and η_0 is an additional constant, initially considered free to be set arbitrarily, and without significant influence on the data fitting capabilities. Later, it turned out that a value of $\eta_0 = (1 - 2\nu)/(1 + \nu)$ was required to obtain a rheology-free damage tensor based on the strain equivalence approach (Carol et al., 1991). Recent results (Carol and Bažant, 1995), indicate that this is actually the condition for the linear elastic model to satisfy the double constraint, i.e. to be simultaneously kinematically and statically constrained (the static constraint means that microplane stresses σ_v , σ_D and σ_T are the projections of the stress tensor σ_{ij} and that, by virtue of the principle of virtual work, the corresponding microplane strains and macroscopic strain tensor also satisfy an integral relation dual to Eq. 2). The double constraint in the elastic model turns out to be a requirement for most developments presented in the following sections. The initial microplane stiffnesses then become:

$$E_v^0 = \frac{E}{1 - 2\nu} \quad ; \quad E_D^0 = E_T^0 = \frac{E}{1 + \nu} \quad (6a, b, c)$$

2.3 Microplane Elasto-Plasticity (MEP)

Elasto-plasticity can be introduced at the microplane level with the following stress-strain relations

$$\sigma_v = E_v^0 (\epsilon_v - \epsilon_v^p) \quad ; \quad \sigma_D = E_D^0 (\epsilon_D - \epsilon_D^p) \quad ; \quad \sigma_T = E_T^0 (\epsilon_T - \epsilon_T^p) \quad (7a, b, c)$$

Substituting (7) into (2), and assuming that the initial moduli satisfy (6) (double constraint), after appropriate manipulation one can obtain (Carol and Bažant, 1995)

$$\sigma_{ij} = E_{ijkl}^0 (\epsilon_{kl} - \epsilon_{kl}^p) \quad (8)$$

$$\epsilon_{ij}^p = \epsilon_v^p \delta_{ij} + \frac{3}{2\pi} \int_{\Omega} \epsilon_D^p n_i n_j d\Omega + \frac{3}{2\pi} \int_{\Omega} \frac{\epsilon_T^p}{2} (n_i \delta_{rj} + n_j \delta_{ri}) d\Omega \quad (9)$$

The repeated indices imply summation except when the indices are within parentheses. Eqs. (8)–(9) represent a classical plastic formulation in which the plastic strain is obtained as the integral of the microplane plastic strains.

2.4 Microplane Elastic Damage (MED)

Alternatively, one can consider elastic-damage relations for the microplane material laws

$$\sigma_v = E_v \epsilon_v \quad ; \quad E_v = \alpha_v E_v^0 \quad (10a, b)$$

$$\sigma_D = E_D \epsilon_D \quad ; \quad E_D = \alpha_D E_D^0 \quad (11a, b)$$

$$\sigma_T = E_T \epsilon_T \quad ; \quad E_T = \alpha_T E_T^0 \quad (12a, b)$$

where α_V , α_D , α_T are some damage coefficients varying from 1 to 0, which can be interpreted geometrically in terms of the undamaged area fractions for each microplane and component. The classical continuum damage theory resorts to the concepts of strain equivalence, energy equivalence or stress equivalence. In the most common strain equivalence approach, the preceding equations can be directly introduced into (2), and assuming that the initial moduli satisfy the double constraint, adequate manipulation leads to the following equations:

$$\sigma_{ij} = E_{ijkl}\epsilon_{kl} \quad ; \quad E_{ijkl} = \alpha_{ijpq} E_{pqkl}^0 \quad (13a, b)$$

$$\begin{aligned} \alpha_{ijpq} = & \frac{\alpha_V}{3} \delta_{ij} \delta_{pq} + \frac{3}{2\pi} \int_{\Omega} \alpha_D n_i n_j (n_p n_q - \frac{\delta_{pq}}{3}) d\Omega + \\ & + \frac{3}{2\pi} \int_{\Omega} \frac{\alpha_T}{4} (n_i n_p \delta_{jq} + n_i n_q \delta_{jp} + n_j n_p \delta_{iq} + n_j n_q \delta_{ip} - 4n_i n_j n_p n_q) d\Omega \end{aligned} \quad (14)$$

i.e., the equations of a classical elastic-damage model in which the fourth-order tensor damage is obtained as an integral of the damage at each microplane (Carol et al., 1991).

The recent results (Carol and Bažant, 1995) include similar developments with the stress equivalence and the energy equivalence approaches. Especially attractive is the energy equivalence approach, in which the final equations obtained (again with the assumption that the elastic model satisfies the double constraint) are

$$\sigma_{ij} = E_{ijkl}\epsilon_{kl} \quad ; \quad E_{ijkl} = \beta_{ijpq} E_{pqrs}^0 \beta_{klrs} \quad (15a, b)$$

$$\begin{aligned} \beta_{ijpq} = & \frac{\sqrt{\alpha_V}}{3} \delta_{ij} \delta_{pq} + \frac{3}{2\pi} \int_{\Omega} \sqrt{\alpha_D} n_i n_j (n_p n_q - \frac{\delta_{pq}}{3}) d\Omega + \\ & + \frac{3}{2\pi} \int_{\Omega} \frac{\sqrt{\alpha_T}}{4} (n_i n_p \delta_{jq} + n_i n_q \delta_{jp} + n_j n_p \delta_{iq} + n_j n_q \delta_{ip} - 4n_i n_j n_p n_q) d\Omega \end{aligned} \quad (16)$$

i.e., the fourth-order damage tensor β_{ijkl} has the same expression as α_{ijkl} except for the square root values of the microplane damage coefficients. In contrast to the strain equivalence approach, the secant stiffness tensor is now guaranteed to exhibit major symmetry even if β_{ijkl} itself as defined in (16) is not. This is a convenient feature for energy consistency of the model, often overlooked in the literature.

2.5 Combination of Microplane Damage and Plasticity (MDP)

Damage and plasticity can be combined by considering microplane laws of the type

$$\sigma_V = E_V(\epsilon_V - \epsilon_V^p) \quad ; \quad \sigma_D = E_D(\epsilon_D - \epsilon_D^p) \quad ; \quad \sigma_T = E_T(\epsilon_T - \epsilon_T^p) \quad (17a, b, c)$$

Assuming double constraint for the elastic model and secant moduli given by (10b-12b), introduction of (17) into (2) and proper manipulation leads to the macroscopic expression

$$\sigma_{ij} = E_{ijkl}(\epsilon_{kl} - \epsilon_{kl}^p) \quad (18)$$

where the plastic strains ϵ_{kl}^p are given in (9), and the secant stiffness E_{ijkl} in (13b,14) with strain equivalence, or in (15b,16) with energy equivalence.

2.6 Discussion and examples

Derivation of damage-related expressions in Sec. 2.4 and 2.5 requires the use of classical concepts in continuum damage mechanics, such as the effective stress and effective strain, which are defined at both macroscopic level (σ_{ij}^{eff} , $\epsilon_{ij}^{\text{eff}}$, $\epsilon_{ij}^{\text{eff},p}$) and microplane level (σ_v^{eff} , σ_D^{eff} , $\sigma_{T_r}^{\text{eff}}$, ϵ_v^{eff} , ϵ_D^{eff} , $\epsilon_{T_r}^{\text{eff}}$, $\epsilon_v^{\text{eff},p}$, $\epsilon_D^{\text{eff},p}$, $\epsilon_{T_r}^{\text{eff},p}$). Further details of these derivations can be found in Carol and Bažant (1995).

Equations for MEP, MED and MDP presented in Sec. 2.3–2.5 are not incompatible with the standard microplane model for concrete of Sec. 2.1. Actually, expressions (4), (7), (10)–(12) and (17) all represent particular cases of the general microplane material laws (3). The kinematic constraint for total nominal strains ϵ_v , ϵ_D and ϵ_{T_r} with ϵ_{ij} , and the corresponding weak form of equilibrium between σ_v , σ_D , σ_{T_r} and σ_{ij} (2) maintain their validity through sections 2.2–2.5, and the specific structure of microplane stress-strain laws in MEP, MED and MDP, together with the double constraint assumed for the underlying elastic model, make it possible to discover additional structures and relations in the formulation, which hold simultaneously with the original kinematic constraint. One consequence is that most examples given in the previous work on the classical microplane model (Bažant and Prat, 1988b; Carol et al., 1992b) can be directly reinterpreted as examples of MEP, MED or MDP formulations. This simply requires rewriting the original stress-strain relations for microplanes (3) in a form similar to (7), (10)–(12) or (17), and extracting the laws for microplane damage (α_v , etc.) or plastic strains (ϵ_v^p , etc.), or both, in terms of the microplane strains (ϵ_v , etc.). Then, calculation of the new integrals (9) and (14) or (16) and the corresponding stresses with (8), (13) or (15) for a specific load history should yield exactly the same results (except for numerical integration and round-off errors) as obtained in the same case with (3) and (2) using the original microplane formulation. This particular exercise was already done in Carol et al. (1991), where a uniaxial compression test was reproduced with an elastic-damage formulation, practically duplicating the same triaxial results as obtained previously with the classical microplane model (Carol et al., 1992b).

Other relevant aspects of the generalized microplane theory with damage and plasticity, including alternative fourth- and second-order damage tensors obtained from the model without normal-deviatoric split, and equivalence of MEP with von Mises and other classical elastoplastic models, can be found in (Carol and Bažant, 1995).

3 Multicrack model *

The multicrack model can be considered an advanced formulation along the line of smeared crack representation initiated with traditional fixed or rotating crack models (Rashid, 1968; Cope et al., 1980; de Borst and Nauta, 1985; Willam et al., 1987; Rots, 1988). Same as some of those models, one assumes an additive decomposition of strain into one contribution from the continuum between the cracks, plus additional contributions from each individual crack:

$$\epsilon = \epsilon^{co} + \sum_{k=1}^N \epsilon_{(k)}^{cr} \quad (19)$$

The normal and shear stresses on each individual crack, σ_N and σ_T , are assumed to be projections of the stress tensor σ_{ij} (static constraint). The continuum between cracks plays the role of the elastic part of the model, while each crack represents an additional plastic mechanism.

3.1 Multisurface elastoplastic description

Each potential crack is represented by a cracking (plastic) surface F , and the corresponding plastic potential Q , hardening variable, etc., all formulated in terms of σ_N , σ_T , ϵ_N^{cr} and ϵ_T^{cr} on the crack plane. The stress components and strain components in the crack plane are grouped into vectors \mathbf{s} and \mathbf{e}^{cr} . Relations with the corresponding macroscopic tensors $\boldsymbol{\sigma}$ and $\boldsymbol{\epsilon}^{cr}$ are based on the static constraint and the principle of virtual work, and so are the derivatives of F and Q , with the expressions

$$\mathbf{s} = \mathbf{N}' \boldsymbol{\sigma} ; \quad \boldsymbol{\epsilon}^{cr} = \mathbf{N} \mathbf{e}^{cr} ; \quad \frac{\partial F}{\partial \boldsymbol{\sigma}} = \mathbf{N} \frac{\partial F}{\partial \mathbf{s}} ; \quad \frac{\partial Q}{\partial \boldsymbol{\sigma}} = \mathbf{N} \frac{\partial Q}{\partial \mathbf{s}} \quad (20a, b, c, d)$$

In 2-D, matrix \mathbf{N} can be written in terms of the angle θ between the normal to the crack plane and the x -axis (de Borst and Nauta, 1985; Rots, 1988; Carol and Prat, 1990)

$$\mathbf{N} = \begin{bmatrix} \cos^2 \theta & -\cos \theta \sin \theta \\ \sin^2 \theta & \cos \theta \sin \theta \\ 2 \cos \theta \sin \theta & \cos^2 \theta - \sin^2 \theta \end{bmatrix} \quad (21)$$

The initial loading surface is a hyperbola in the σ_N - σ_T space with tensile strength $\chi_0 = f'_t$, asymptotically equivalent to a Mohr-Coulomb surface defined by c and $\tan \phi$. The plastic flow is associated in tension, and dilatancy is reduced in compression, vanishing for $|\sigma_N| \geq \sigma^{dil}$. Softening laws are governed by w^{cr} (fracture work), equal to the plastic work in tension, and to its tangential part, friction excluded, in compression. With cracking,

* This section is authored by I. Carol.

χ decreases, vanishing for $w^{cr} = g_f^I =$ mode I fracture energy. c decreases more slowly, vanishing for $w^{cr} = g_f^{IIa} =$ fracture energy in mode IIa, normally larger than g_f^I . Mode IIa is defined as a limit situation with shear and no dilatancy (i.e. high compression). At $w^{cr} = g_f^I$, the hyperbola changes little, but its tip is shifted to the origin. At $w^{cr} = g_f^{IIa}$, it degenerates into a pair of straight lines representing pure friction. More details of the model for a single crack can be found in (Carol et al., 1993; Carol and Prat, 1995).

Assuming N cracks simultaneously satisfying $F = 0$ (corner situation), the elastoplastic rate equations are

$$\dot{\boldsymbol{\sigma}} = \mathbf{E}^{co} \left(\dot{\boldsymbol{\epsilon}} - \sum_{i=1}^N \dot{\boldsymbol{\epsilon}}_{(i)}^{cr} \right) \quad (22)$$

$$\dot{\boldsymbol{\epsilon}}_{(i)}^{cr} = \dot{\lambda}_{(i)} \frac{\partial Q_{(i)}}{\partial \boldsymbol{\sigma}} ; \quad i = 1, N \quad (23)$$

$$\dot{F}_{(i)} = \left[\frac{\partial F_{(i)}}{\partial \boldsymbol{\sigma}} \right]^t \dot{\boldsymbol{\sigma}} - \sum_{j=1}^N H_{(i,j)} \dot{\lambda}_{(j)} ; \quad i = 1, N \quad (24)$$

where $H_{(i,j)}$ are the hardening-softening parameters which, in this case, are defined as

$$H_{(i,i)} = - \frac{\partial F_{(i)}}{\partial \lambda_{(i)}} = - \frac{\partial F_{(i)}}{\partial \mathbf{p}_{(i)}} \frac{\partial \mathbf{p}_{(i)}}{\partial w_{(i)}^{cr}} \frac{\partial w_{(i)}^{cr}}{\partial \boldsymbol{\epsilon}_{(i)}^{cr}} \frac{\partial Q_{(i)}}{\partial \boldsymbol{\sigma}} \quad (25a, b)$$

$$H_{(i,j)} = - \frac{\partial F_{(i)}}{\partial \lambda_{(j)}} = 0 \quad \text{for } i \neq j$$

In (25a), \mathbf{p} are the vectors with the surface parameters which change with hardening-softening; in this case $\mathbf{p} = [\chi, c]^t$ for each surface. With these definitions, $H_{(i,j)}$ is diagonal and its terms are always negative, i.e. one has a purely softening law uncoupled between the various surfaces.

3.2 The infinitesimal corner problem and tangential stiffness

At a corner with N crack surfaces, equations (22)–(24) can be combined to obtain

$$\begin{bmatrix} -\dot{F}_{(1)} \\ -\dot{F}_{(2)} \\ \vdots \\ -\dot{F}_{(N)} \end{bmatrix} = \begin{bmatrix} \bar{H}_{(1,1)} & \bar{H}_{(1,2)} & \dots & \bar{H}_{(1,N)} \\ \bar{H}_{(2,1)} & \bar{H}_{(2,2)} & \dots & \bar{H}_{(2,N)} \\ \vdots & \vdots & \ddots & \vdots \\ \bar{H}_{(N,1)} & \bar{H}_{(N,2)} & \dots & \bar{H}_{(N,N)} \end{bmatrix} \begin{bmatrix} \dot{\lambda}_{(1)} \\ \dot{\lambda}_{(2)} \\ \vdots \\ \dot{\lambda}_{(N)} \end{bmatrix} + \begin{bmatrix} B_{(1)} \\ B_{(2)} \\ \vdots \\ B_{(N)} \end{bmatrix} \quad (26)$$

where the matrix and the right-hand side vector are known in advance

$$\bar{H}_{(i,j)} = H_{(i,j)} + \left[\frac{\partial F_{(i)}}{\partial \boldsymbol{\sigma}} \right]^t \mathbf{E}^{co} \frac{\partial Q_{(j)}}{\partial \boldsymbol{\sigma}} , \quad B_{(i)} = - \left[\frac{\partial F_{(i)}}{\partial \boldsymbol{\sigma}} \right]^t \mathbf{E}^{co} \dot{\boldsymbol{\epsilon}} \quad (27a, b)$$

Eqs. (22)–(24) must be complemented with loading/unloading conditions: for each row in (26), either $\dot{\lambda}$ is positive with $\dot{F} = 0$ (plastic loading), or $\dot{\lambda} = 0$ with $\dot{F} \leq 0$ (elastic unloading). Determination of the subset of active surfaces is not trivial, requiring in general an iterative procedure, as for instance the one described in the next section.

Assuming now that the subset of N_{ac} active surfaces is known, and that $\bar{G}_{(i,j)}$ is the inverse of the reduced matrix $\bar{H}_{(i,j)}$ with only rows and columns corresponding to active surfaces, the plastic multipliers and tangential stiffness can be obtained

$$\dot{\lambda}_{(i)} = - \sum_{j=1}^{N_{ac}} \bar{G}_{(i,j)} \left[\frac{\partial F_{(i)}}{\partial \sigma} \right]^t \mathbf{E}^{co} \dot{\epsilon} ; \quad i = 1, N_{ac} \quad (28)$$

$$\dot{\sigma} = \mathbf{E}^{tan} \dot{\epsilon} ; \quad \mathbf{E}^{tan} = \mathbf{E}^{co} - \sum_{i=1}^{N_{ac}} \sum_{j=1}^{N_{ac}} \bar{G}_{(i,j)} \mathbf{E}^{co} \frac{\partial Q_{(i)}}{\partial \sigma} \otimes \left[\frac{\partial F_{(j)}}{\partial \sigma} \right]^t \mathbf{E}^{co} \quad (29a, b)$$

3.2 Numerical implementation

The model has been implemented in 2-D in combination with linear elasticity. Possibilities of cracking have been restricted to 12 predetermined directions, which are equally spaced every 15° across the upper semicircle. Although similar developments have been proposed recently without these restrictions (Weihe et al., 1994), a fixed selection of predefined potential crack directions can be considered analogous to the restriction that cracking in a finite element can only occur at the integration points; if enough directions are considered, it does not pose a severe restriction on the cracking modes, and in exchange it is a way to circumvent a number of practical problems that otherwise arise in the implementation of the model.

The computer routine for constitutive verification follows a scheme similar to that proposed in Carol et al. (1992b) for the microplane model, with a strain-driven constitutive subroutine, managed from a 1-point main program that iterates according to a Newton scheme only on those degrees of freedom with prescribed stresses. The constitutive subroutine is mainly based on the calculation of new contact-deactivation points, a crucial aspect in this type of model with many loading surfaces. While the number of active surfaces remains constant, the increment of prescribed strain is divided into subincrements, and for each of them a trapezoidal rule is applied iteratively to integrate the plastic equations. If changes in the set of active surfaces are detected at the end of the subincrement, the earliest contact/deactivation point is obtained, and the subincrement size is reduced accordingly for the next iteration. In this way, upon convergence of the process, the contact point will be reached precisely.

Once a contact-deactivation point involving more than one surface (i.e. a corner point) has been reached, an iterative procedure is initiated to determine the precise set of active surfaces for the following subincrement. The

active set of surfaces must be a subset of the total number of surfaces at the corner. In the first iteration, all the surfaces involved are assumed active. The entire left-hand side vector in (25) is therefore null, and the system can be solved to obtain the plastic multipliers. If one or more multipliers obtained are negative, those surfaces are dropped, the corresponding rows and columns are eliminated from the system, and a new solution for the multipliers is obtained. In the second and further iterations, the verification that all surfaces assumed inactive are really in that state is also required. This consists of simply calculating the corresponding left-hand term in (25) and checking its positiveness. Otherwise, the surface must be reincorporated into the active set for the subsequent iteration (this second verification was not stated clearly in the earlier algorithms proposed (Simó et al., 1988)). More details of the numerical implementation with discussion of additional difficulties that may arise during calculations can be found in Carol and Prat (1995).

3.3 Willam's test with rotation of principal directions

The multicrack model described was demonstrated in the past for examples in tension, compression and shear, without rotation of principal directions (Carol et al., 1993). Recent results include a numerical test with significant rotations of principal stresses (Willam et al., 1987), in which a correct performance of the the corner algorithm is required in order to get a consistent solution. In this test, uniaxial tension is applied first in the x direction, reaching the onset of tensile cracking. Subsequent strain increments are prescribed to all degrees of freedom proportionally to $\Delta\epsilon = [\Delta\epsilon_{xx}, \Delta\epsilon_{yy}, \Delta\gamma_{xy}]^t = [0.50, 0.75, 1.00]^t$. This implies increments of tensile strain for both principal axes, accompanied by a rotation that reaches asymptotically the value of 38° . The parameters used are: $E = 10,000\text{MPa}$, $\nu = 0.18$, $\tan\phi = 0.8785$, $f'_t = 1.0\text{MPa}$, $c_0 = 1.5\text{MPa}$, $g_f^I = 0.00015\text{MPa}$, $g_f^{IIa} = 0.0015\text{MPa}$, $\sigma^{\text{dil}} = 1,000\text{MPa}$, and $\alpha_x = \alpha_c = 0$. The crack orientations are numbered 1 to 12 starting counter-clockwise from the normal along the x -axis. The evolution of σ_{xx} (equal to $\sigma_{N(1)}$) and σ_{xy} (equal to $\sigma_{T(1)}$) is represented in Fig. 1. Changes in crack status are indicated with a vertical line and +, - or = followed by crack number.

The first load step shows a linear increase of the normal stress reaching the initial tensile strength, with zero shear stresses. At that point, crack 1 is activated. With the second load step, the normal strain continues to increase on plane 1 with decreasing stress (softening), although now accompanied by an increasing amount of shear strain, which causes the shear stresses to build up. At the same time, the strains (and stresses) begin to increase in other planes, until a corner point is reached involving planes 1 and 5 (60° apart from the initial crack). The corner situation is resolved with crack 5 opened and crack 1 deactivated. After that, σ_{xx} initially continues decreasing (now in unloading regime rather than softening), although shortly after that the tendency is inverted and the cracking surface for plane 1 is reached again,

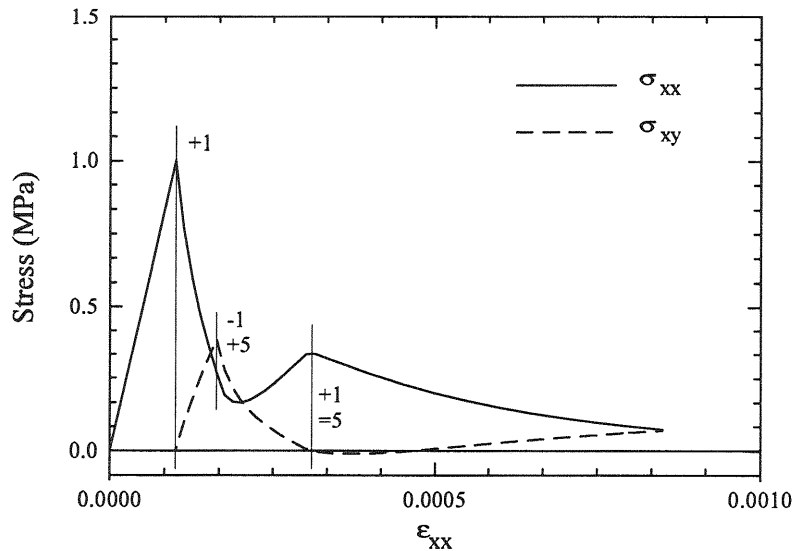


Fig. 1 — Willam's test in rotating tension/shear

with a new corner point involving the same surfaces 1 and 5. This second time, however, the corner is resolved with both cracks remaining active, and this situation is maintained for the rest of the test, with stresses slowly vanishing in all directions.

3.4 Discussion

In the example presented, the multicrack model seems capable of handling complex crack states with non-trivial corner situations. The model exhibits a natural shielding effect of the first crack onto neighbor directions of potential cracking, without the need of introducing ad hoc threshold angle parameters. This is apparent from the fact that the second crack opens at 60° , even if strains prescribed are tensile and continuously increasing in all directions around the first crack. The shielding effect can be explained from the static constraint and the softening laws, since stresses on plane 1 decrease fast after first cracking, "taking back" with them also the stresses in neighboring planes which must lie nearby on the same Mohr circle. This adds to all previous features of multicrack model such as a consistent definition of the second mode of fracture, a reduced set of parameters including fracture energies, etc. All these advantages are, however, at the price of dealing with a 12-surface elastoplastic model, still posing theoretical and computational challenges to be addressed in the future. Further discussion and details on the model can be found in (Carol and Prat, 1995; Carol et al., 1995).

4 Concluding remarks

The two models presented, microplane and multicrack, represent different aspects of concrete behavior. The microplane model with kinematic constraint seems more naturally adapted to the behavior before severe lo-

calization takes place, while the multicrock model specializes precisely in that situation. Although the available results for the multicrock model have so far been obtained only in conjunction with linear elasticity, any model could be used for that purpose, and in particular the possibility of combining microplane and multicrock models in a single formulation seems a very attractive possibility to be explored in the future.

Acknowledgements

Partial support from DGICYT (Madrid, Spain) under research grants PB92-0702 and PB93-0955 is gratefully acknowledged.

References

- Batdorf, S. and Budiansky, B. (1949). A mathematical theory of plasticity based on the concept of slip. Technical Note 1871, National Advisory Committee for Aeronautics.
- Bažant, Z. and Gambarova, P. (1984). Crack shear in concrete: crack band microplane model. *J. Struct. Engng. ASCE*, 110:2015–2035.
- Bažant, Z., Jirásek, M., Xiang, Y., and Prat, P. (1994). Microplane model with stress-strain boundaries and its identification from tests with localized damage. In Mang, H., Bićanić, N., and de Borst, R., editors, *Computational modelling of concrete structures*, pages 255–261, Innsbruck. Pineridge Press.
- Bažant, Z. and Oh, B. (1983). Microplane model for fracture analysis of concrete structures. In U.S. Air Force Academy, editor, *Proc. Symp. on the Interaction of Non-Nuclear Munitions with Structures*, pages 49–55, Colorado Springs.
- Bažant, Z. and Oh, B. (1985). Microplane model for progressive fracture of concrete and rock. *J. Engng. Mech. ASCE*, 111:559–582.
- Bažant, Z. and Ožbolt, J. (1990). Non-local microplane model for fracture, damage and size effect in structures. *J. Engng. Mech. ASCE*, 116:2485–2504.
- Bažant, Z. and Prat, P. (1988a). Microplane model for brittle-plastic material: I. Theory. *J. Engng. Mech. ASCE*, 114(10):1672–1688.
- Bažant, Z. and Prat, P. (1988b). Microplane model for brittle-plastic material: II. Verification. *J. Engng. Mech. ASCE*, 114(10):1689–1702.
- Bažant, Z., Xiang, Y., and Prat, P. (1995). Microplane for concrete: I. Stress-

- strain boundaries and finite strain. *J. Engng. Mech. ASCE*, 121:(in press).
- Carol, I. and Bažant, Z. (1991). Damage-rheology uncoupling for microplane damage tensor, with application to concrete with creep. In Desai, C., Krempl, E., Frantziskonis, G., and Saadatmanesh, H., editors, *Constitutive laws for engineering materials*, pages 391–394, Tucson, U.S.A. ASME Press.
- Carol, I. and Bažant, Z. (1995). Damage and plasticity in microplane theory. Joint Report (in preparation), ETSECCPB-UPC and Dept. of Civil Engineering, Northwestern University.
- Carol, I., Bažant, Z., and Prat, P. (1991). Geometric damage tensor based on microplane model. *J. Engng. Mech. ASCE*, 117:2429–2448.
- Carol, I., Bažant, Z., and Prat, P. (1992a). Microplane-type constitutive models for distributed damage and localized cracking in concrete structures. In Bažant, Z., editor, *Fracture Mechanics of Concrete Structures (FraMCoS I)*, pages 299–304, Breckenridge, Colorado, USA. Elsevier.
- Carol, I. and Prat, P. (1990). A statically constrained microplane model for the smeared analysis of concrete cracking. In Bićanić, N. and Mang, H., editors, *Computer aided analysis and design of concrete structures*, volume 2, pages 919–930, Zell-am-See, Austria. Pineridge Press.
- Carol, I. and Prat, P. (1991). Smeared analysis of concrete fracture using a microplane based multicroack model with static constraint. In van Mier, J., Rots, J., and Bakker, A., editors, *Fracture processes in concrete, rock and ceramics*, pages 619–628, Noordwijk, The Netherlands. E & FN SPON.
- Carol, I. and Prat, P. (1995). A multicroack model based on the theory of multisurface plasticity and two fracture energies. In Owen, D., Oñate, E., and Hinton, E., editors, *Computational Plasticity (COMPLAS IV)*, volume 2, pages 1583–1594, Barcelona. Pineridge Press.
- Carol, I., Prat, P., and Bažant, Z. (1992b). New explicit microplane model for concrete: theoretical aspects and numerical implementation. *Int. J. Solids and Structures*, 29(9):1173–1191.
- Carol, I., Prat, P., and Gettu, R. (1993). Numerical analysis of mixed-mode fracture of quasi-brittle materials using a multicroack constitutive model. In Rossmannith, H. and Miller, K., editors, *Mixed-mode fatigue and fracture*, pages 319–332. Mechanical Engineering Publications Ltd., London. ESIS Publication 14.
- Carol, I., Prat, P., López, C., and Gettu, R. (1995). A normal/shear cracking model for quasi-brittle materials. I: Interface implementation for discrete fracture analysis, and II: Multicroack implementation for smeared fracture analysis. Technical Report in preparation, ETSECCPB-UPC, E-08034 Barcelona (Spain).
- Cope, R., Rao, P., Clark, L., and Norris, P. (1980). Modelling of reinforced

- concrete behavior for finite element analysis of bridge slabs. In Taylor, C. et al., editors, *Numerical Methods for Non-linear Problems 1*, pages 457–470, Swansea, UK. Pineridge Press.
- de Borst, R. and Nauta, P. (1985). Non-orthogonal cracks in a smeared finite element model. *Engng. Comput.*, 2:35–46.
- Mohr, O. (1900). Welche Umstände bedingen der Bruch und der Elastizitätsgrenze des Materials. *Z. Vereins Deutscher Ingenieure*, 1524.
- Pande, G. and Sharma, K. (1983). Multilaminate model of clays — A numerical evaluation of the influence of rotation of principal axes. *J. Engng. Mech. ASCE*, 109(7):397–418.
- Rashid, Y. (1968). Analysis of prestressed concrete pressure vessels. *Nuclear Engineering and Design*, 7:334–344.
- Rots, J. (1988). *Computational modelling of concrete fracture*. PhD thesis, Delft University of Technology, The Netherlands.
- Simó, J., Kennedy, J., and Govindjee, S. (1988). Non-smooth multisurface plasticity and viscoplasticity. Loading/unloading conditions and numerical algorithms. *Int. J. Num. Methods in Engineering*, 26:2161–2185.
- Taylor, G. (1938). Plastic strain in metals. *J. Inst. Metals*, 62:307–324.
- Weihe, S., Koenig, M., and Kroeplin, B. (1994). A treatment of mixed mode fracture in debonding. *Comp. Mat. Sci.*, 3:254–262.
- Willam, K., Pramono, E., and Sture, S. (1987). Fundamental issues of smeared crack models. In Shah, S. and Swartz, S., editors, *SEM-RILEM Int. Conf. on Fracture of Concrete and Rock*, pages 192–207, Bethel. SEM.
- Zienkiewicz, O. and Pande, G. (1977). Time-dependent multi-laminate model of rocks — A numerical study of deformation and failure of rock masses. *Int. J. Num. Anal. Methods in Geomechanics*, 1:219–247.

